

DIVIDING ANNULAR FLOW IN A HORIZONTAL TEE

J. A. R. HENRY

Heat Transfer & Fluid Flow Service, National Engineering Laboratory, East Kilbride, Glasgow, Scotland

(Received 12 May 1980; in revised form 11 December 1980)

Abstract—The prediction of mixture composition in a branch from a manifold in which two-phase mixtures flow has been examined. A linear relationship is found to exist between the branch mass flowrates of the individual phases over a range of flow conditions. This observation is used as the basis of a correlation which contains coefficients that are functions of the manifold flow condition. 90 per cent of the data are correlated to within ± 20 per cent.

1. INTRODUCTION

Many occasions arise in practice when it is desired to distribute a mixture of gas (or vapour) and liquid through a pipe network containing branches. Usually the aim is to divide the gas and liquid uniformly throughout the system, and is essential for obtaining balanced operation of plant, which in turn results in increased utilization. The pipe network often takes the form of a manifold.

On other occasions, it is necessary to predict the degree of maldistribution which results when a two-phase mixture flows through a pipe network as, for example, happens during accident conditions in certain types of plant.

Both of these cases involve designers being able to predict the behaviour of flow through a junction, under two-phase conditions. In spite of the importance of this subject there has been relatively little effort spent in pursuing it experimentally, the most important contributions being from Tsuyana & Taya (1959), Fouda (1970), Fouda & Rhodes (1972, 1974) and Honan & Lahey (1978). The approach of these workers has been similar to that adopted for single-phase dividing flow and it is therefore relevant to consider briefly the background.

2. DIVIDING SINGLE-PHASE FLOW

Dow (1950), Acrivos *et al.* (1959) and Idelchik & Shteinberg (1974) have studied the design and prediction of single-phase networks and manifolds and the state of the art is now such that acceptably accurate calculations can be performed in many cases. Martin & Peters (1963) have developed computer methods for solving the often complex set of equations which result and Martin & Tee (1961) have written computer programs which address themselves to this particular problem.

Such a solution depends on the knowledge of the pressure drop characteristics of every component in the network. These characteristics can take the form

$$\Delta p = K\rho U^n \quad [1]$$

in which K and n are constants in a particular situation.

Where the flow encounters a change in flow area there is also a change in momentum flux due to the velocity change. Both of these effects are present in a pipe branch and may be represented by the following equations.

Considering flow through the simple T-piece shown in figure 1, the pressure change in the main flow direction (1-2) may be represented by an equation of the form

$$p_2 - p_1 = K_M \rho (U_1^2 - U_2^2) \quad [2]$$

where the momentum recovery factor K_M allows for the failure of the side stream to leave the dotted control volume perpendicular to the main flow direction.

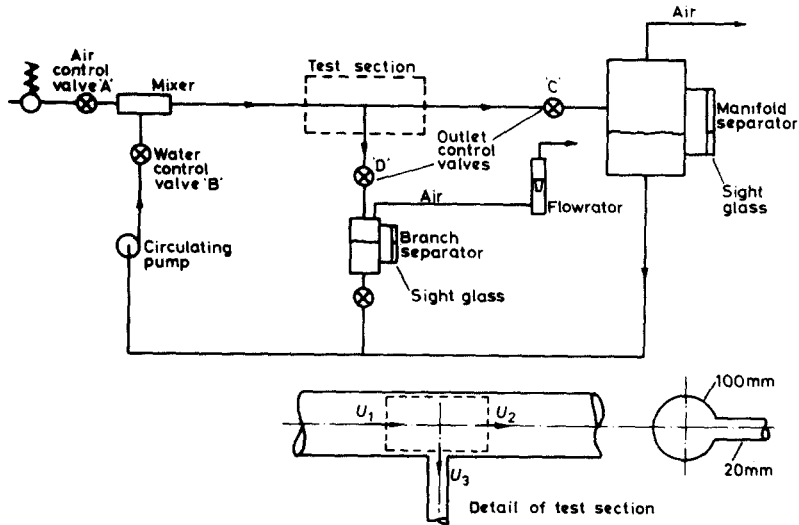


Figure 1. Test circuit.

The pressure change experienced by the fluid entering the branch (U_3) may be represented by

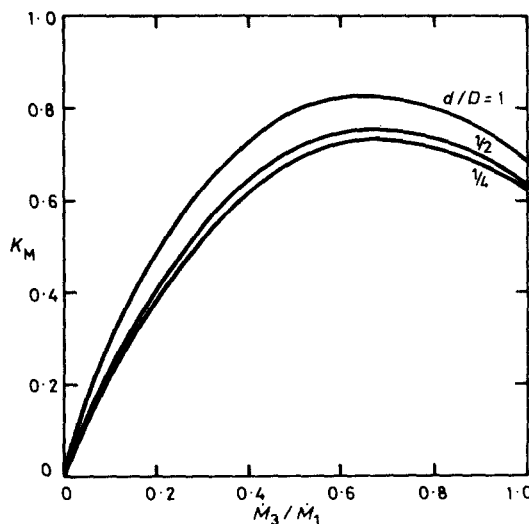
$$p_1 - p_3 = K_S \rho \frac{U_3^2}{2} \quad [3]$$

where K_S is the side-stream loss coefficient.

Values of K_M and K_S may be found from figures 2 and 3. Research into single-phase distribution has therefore largely concerned itself with the study of flow through various geometries of branch in order to obtain values for the empirical constants K_M and K_S , as for example was done by Hoopes *et al.* (1948), Dow (1950), McNown & Hus (1951) and McNown (1954).

3. DIVIDING TWO-PHASE FLOW

In order to predict the behaviour of two-phase flow at a branch, a procedure similar to that just described has been followed by Tsuyana & Taya (1959), Fouda (1970) and Fouda & Rhodes

Figure 2. Momentum coefficient K_M for single phase dividing flow, Dow (1950).

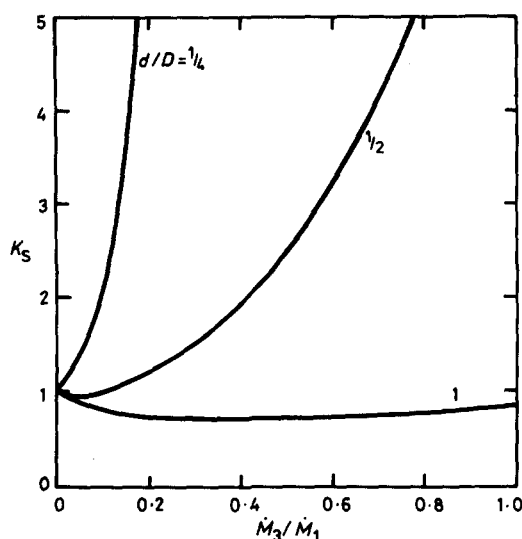


Figure 3. Branch loss coefficient K_S for single phase dividing flow, Dow (1950).

(1972, 1974) who carried out experiments to determine the loss coefficients K_M and K_S . Such tests however tell little about the manner in which the phases redistribute themselves at the branch. Each phase experiences the same pressure difference between any two stations, and the resulting behaviour when, for example, a branch is encountered depends critically on the phase distribution (flow pattern) within the manifold upstream of the branch. Phase division is not a strong function of pressure gradients within the T-piece, and it is therefore suggested that an essential part of any solution method for a two-phase pipe network must be a relationship between the branch phase flowrates and those in the upstream manifold, which does not include local pressure gradient, i.e.

$$(\dot{M}_{G3}, \dot{M}_{L3}) = f(\dot{M}_G, \dot{M}_{L1}). \quad [4]$$

Equation [4] may be rewritten in a form which is more convenient, and also more significant, yet retains its essential features.

$$x_3 = f(\dot{M}_1, x_1, r_3). \quad [5]$$

Alongside such a relationship, correlations for the pressure changes within the T-piece are of relatively secondary importance.

For this reason, the whole objective of the NEL experiments has been to demonstrate the existence of a relationship such as [5] and to derive what its likely form may be.

4. EXPERIMENTAL RESULTS

A test loop was constructed at NEL as shown in figure 1, in which air and water were mixed and passed through the test section consisting of a transparent manifold of i.d. 100 mm, with a branch of i.d. 20 mm, i.e. $d/D = 1/5$. Both the manifold and the branch were horizontal, and all tests were carried out at nominally ambient pressure and temperature.

The mixer is a sintered metal sleeve with the water entering radially to mix with the air thus favouring annular flow patterns.

The distance between the mixer and the T-piece is 30 manifold diameters, and, while this is too short for equilibrium to be obtained, at least reflects the conditions likely to be obtained in practice. In future work it would be essential to obtain local liquid film and entrainment measurements immediately upstream of the T-piece and to relate its behaviour to these.

The procedure was to set up the desired manifold water and air flows using valves *A* and *B*. The branch valve *D* was then opened in a series of stages, at each of which valve *C* was used to maintain the test section pressure constant, at a level slightly above atmospheric. At each stage the branch air and water flowrates were noted, and these are plotted for some typical tests in figure 4. At most, approx. 6 per cent of the total flow was removed through the branch. Figure 4 shows the typical effect on division of each phase of manifold quality while the mass velocity in the manifold is held constant. It is apparent that the branch liquid flowrate (or mass velocity) varies approximately linearly with the branch gas flowrate (or mass velocity), that is

$$\dot{M}_{L3} = \dot{M}_i + S\dot{M}_{G3} \quad [6]$$

where \dot{M}_i and S are constants for given manifold conditions.

Figure 5 shows the way in which branch quality typically varies with branch flowrate, and also shows the effect of manifold mass velocity. It is apparent that for these data:

(a) Branch quality eventually levels out to a certain value. The branch flowrate at which this happens is approximately proportional to the manifold mass velocity \dot{m}_1 (it is clear however that, when $\dot{M}_3 = \dot{M}_1$, then $x_3 = x_1$).

(b) Ideal phase split is more likely to be obtained with a high mass velocity in the manifold. Low mass velocity results in severe maldistribution with air preferentially leaving the manifold for the geometry considered here. To a certain extent this is supported by experience.

If the data collected are cross-plotted, the result is as figure 6 and shows directly and emphatically the manner in which branch quality and manifold quality behave relative to each other. It is clear that the flow division could hardly be further from the ideal: in general the T-piece characteristic intersects the ideal characteristic at right angles.

The shape of the entire T-piece characteristic can be reasoned to be perhaps as shown in figure 7. Segment O-A of the characteristic is the least well defined since it depends on the position of the liquid surface relative to the branch. If the liquid flowrate is large the branch may flow full of liquid, but if the liquid flowrate is small the branch may flow full of gas. Segment A-B is a more predictable region and observation has indicated that it corresponds to

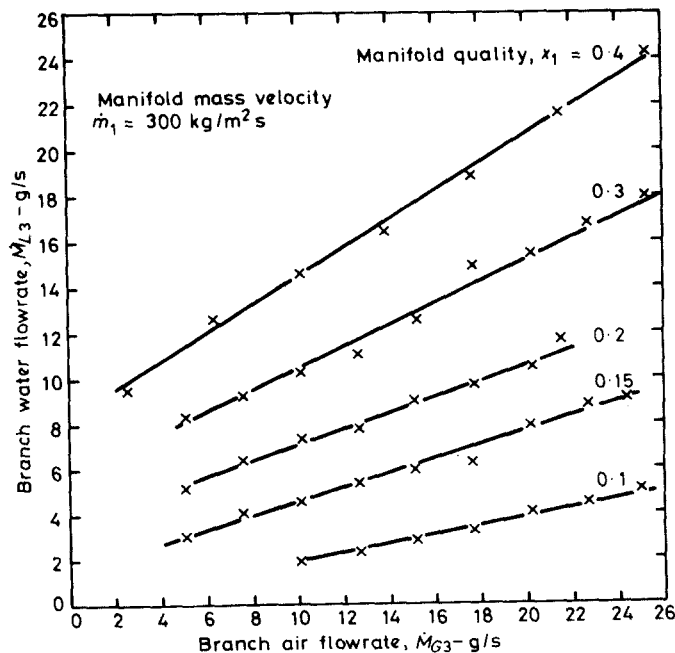


Figure 4. Typical test results; effect of quality.

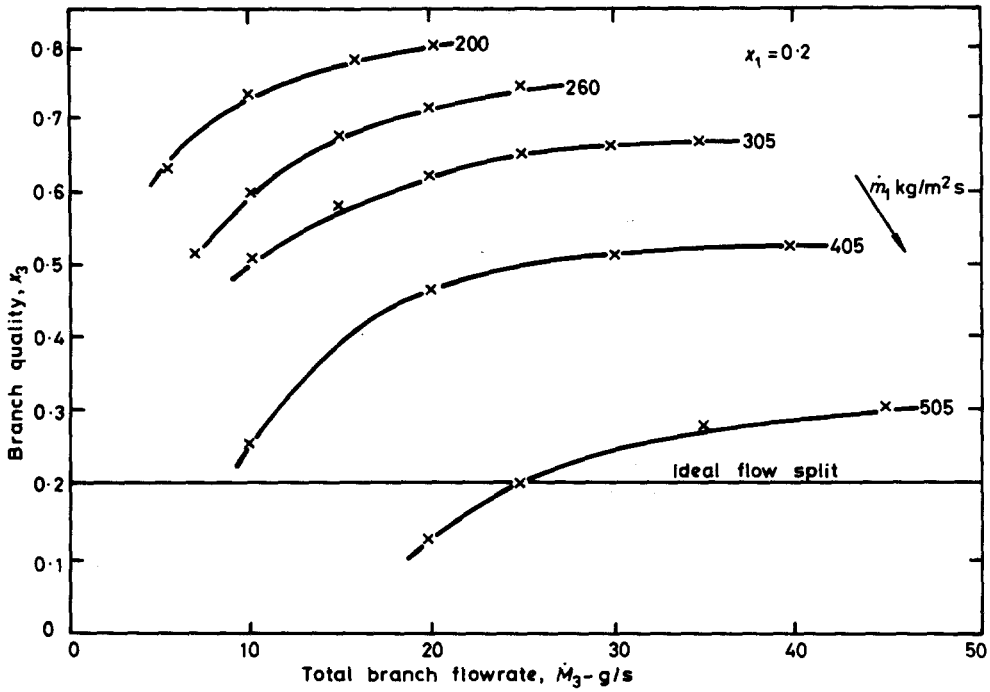


Figure 5. Typical variation of branch quality with branch flowrate (constant $x_1 = 0.2$, varying \dot{m}_1).

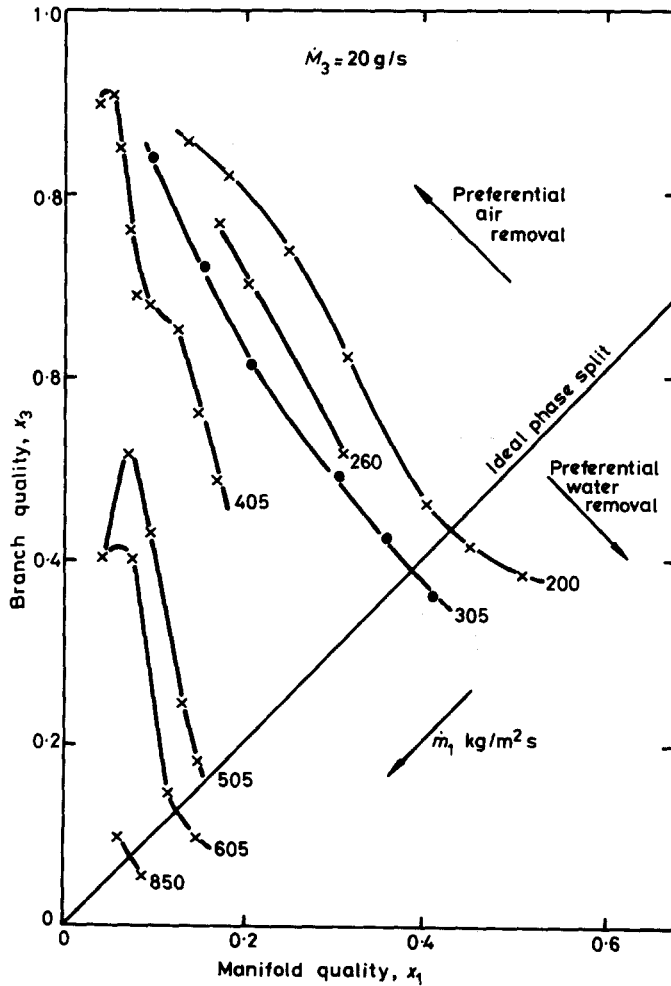


Figure 6. Variation of branch quality with manifold quality ($\dot{M}_3 = 20 \text{ g/s} = \text{constant}$).

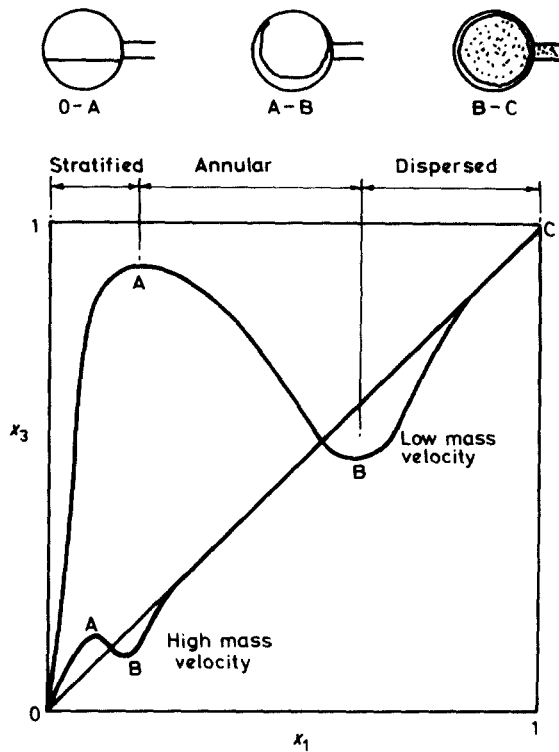


Figure 7. Significance of figure 6 in terms of flow pattern: branch flow held constant.

the transition to the annular type of flow pattern from the stratified. Most of the data reported here are for this region as shown in figures 6 and 8. Segment B-C corresponds to the onset of entrainment of the liquid film into the gas phase, with corresponding improvement in the T-piece characteristic as the flow becomes more homogeneous, and eventually asymptotic to the ideal characteristic.

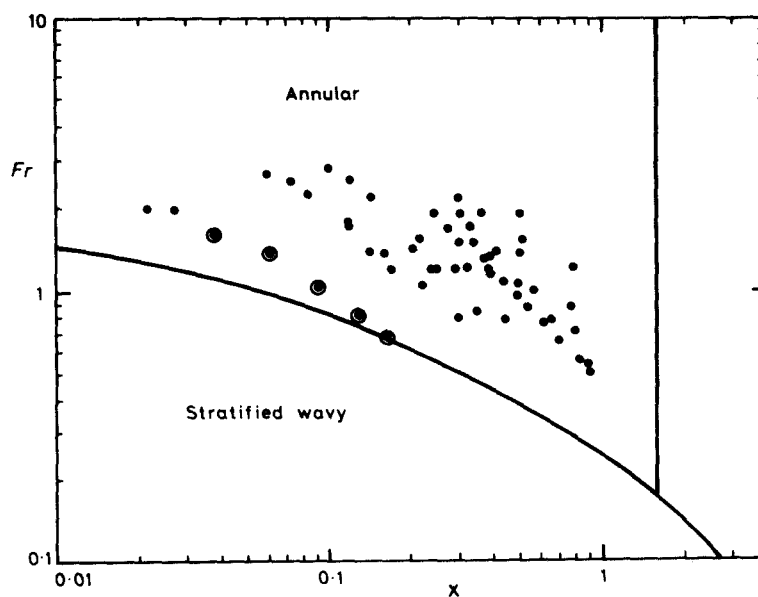


Figure 8. Position of data on the Taitel Dukler (1976) map. (Circled points correspond to those on figures 9 and 10.)

Wallis (1969) gives an expression for the equilibrium entrainment based on a dimensionless gas velocity

$$\pi_2 = \frac{U_G \mu_G}{\sigma} \left(\frac{\rho_G}{\rho_L} \right)^{1/2}. \quad [7]$$

For the conditions at which the NEL data were collected

$$\pi_2 = 6.5 \times 10^{-6} \dot{m}_1 x_1,$$

and it is perhaps of interest to note that the location of the minimum points B (see figure 7) for the data shown in figure 6 given approximately by

$$\dot{m}_1 x_1 = 110 \quad [8]$$

which corresponds to approx. 50 per cent entrainment. It was however pointed out that the NEL test section has a very short upstream settling length (30 manifold diameters) so that the flow had not reached an equilibrium state.

At high mass velocity the departure from the ideal characteristic might be expected to be less severe and to occur at lower quality as indicated on figure 7 and verified by figure 6.

5. METHOD OF ANALYSIS

Since, by definition quality is

$$x_3 = \frac{\dot{M}_{G3}}{\dot{M}_{G3} + \dot{M}_{L3}} = \frac{\dot{M}_{G3}}{\dot{M}_3} \quad [9]$$

substituting [6] into [9] and using mass velocity rather than mass flowrate gives

$$x_3 = \frac{1}{S+1} \left(1 - \frac{\dot{m}_1}{\dot{m}_3} \right). \quad [10]$$

Equation [10] is the relationship previously described by [5] and relates the branch quality x_3 to the branch mass velocity \dot{m}_3 using the parameters \dot{m}_1 and S which, from [5], might be expected to be functions of \dot{m}_1 and x_1 , i.e.

$$\dot{m}_1 = f_1(\dot{m}_1, x_1) \quad [11]$$

and

$$S = f_2(\dot{m}_1, x_1). \quad [12]$$

Equation [10] also shows that the value to which x_3 will tend at high branch flowrate ($\dot{M}_3 \gg \dot{M}_1$) is

$$x_3 = \frac{1}{S+1}. \quad [13]$$

It is clear that x_3 will tend to x_1 at high values of branch flowrate; this presumably represents the breakdown of the straight line relationship represented by [6] as for example reported by Collier (1976).

A sample of the data collected was examined and the best least mean squares fit method used to obtain the values of \dot{m}_i and S for each set of manifold conditions. Examination of these parameters revealed that an approximate correlation could be obtained if plotted as follows

$$S\left(\frac{x_1}{1-x_1}\right) = f(\dot{m}_{G1}) \tag{14}$$

$$\dot{m}_i\left(\frac{x_1}{1-x_1}\right) = f(\dot{m}_{G1}). \tag{15}$$

This is shown in figures 9 and 10, which also have been represented by an empirical fit, as follows

$$S\left(\frac{x_1}{1-x_1}\right) = 8.1 \times 10^{-7} \dot{m}_{G1}^3 \tag{16}$$

$$\dot{m}_i\left(\frac{x_1}{1-x_1}\right) = 0.00007(\dot{m}_{G1} - 10)^3. \tag{17}$$

The circled points in each figure clearly do not follow the trend of the rest of the data and from observation correspond to a more stratified type of flow pattern, which as already discussed, appears to be associated with region O-A of figure 7. With a stratified flow pattern, it can be argued that the amount of liquid entering the branch, and hence the branch quality, will be related to the liquid depth in the manifold; Taitel & Dukler (1976) have shown this is related to the Lockhart-Martinelli parameter. The point of maximum branch quality (point A in figure 7) appears to occur, from figure 6, at a value of $x_1 = 0.05$; for x less than this value the limited data available are correlated approximately by

$$\dot{m}_i = 544 - 491X. \tag{18}$$

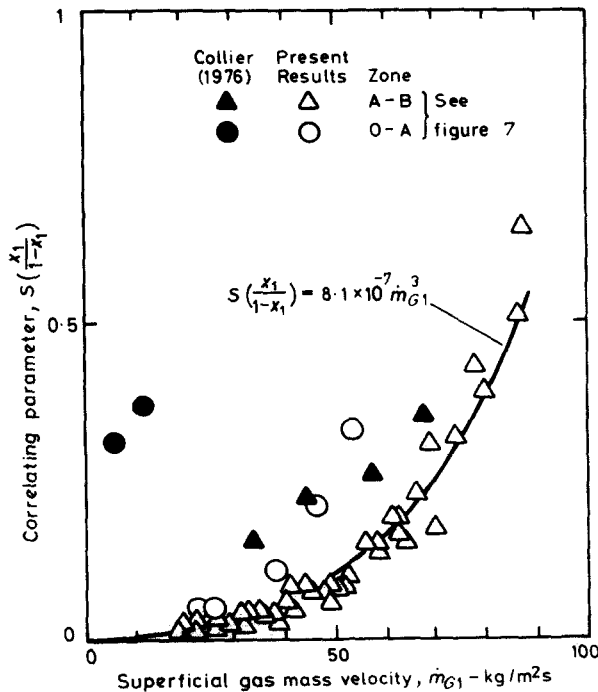


Figure 9. Correlation of $Sx_1/(1-x_1)$ with \dot{m}_{GL} .

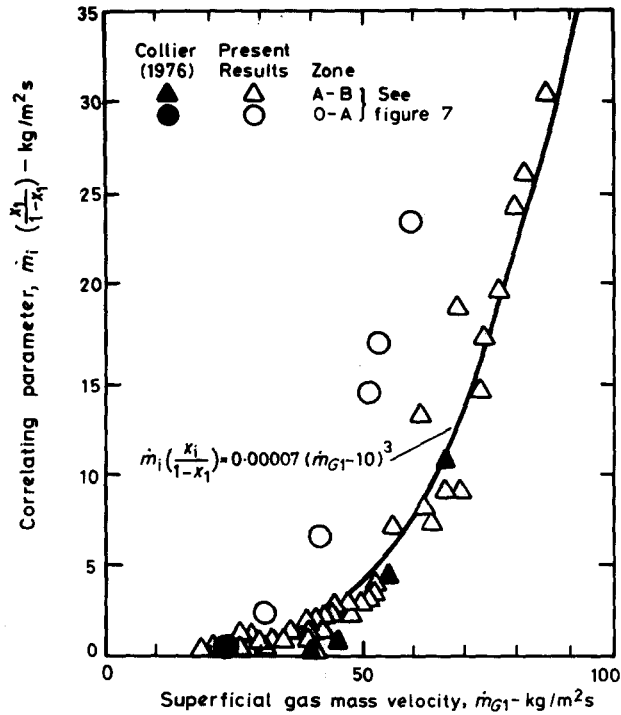


Figure 10. Correlation of $\dot{m}_i x_i / (1 - x_i)$ with \dot{m}_{GL} .

For the complete NEL data, values of branch quality were calculated by [10] using [16]–[18] as appropriate. These are compared with the measured values figure 11, and agreement is seen to be reasonable considering the sensitivity of the analysis to error and the simplicity of method of correlation. Figure 11(a) shows the agreement for all data collected, and figure 11(b) shows agreement for a typical run.

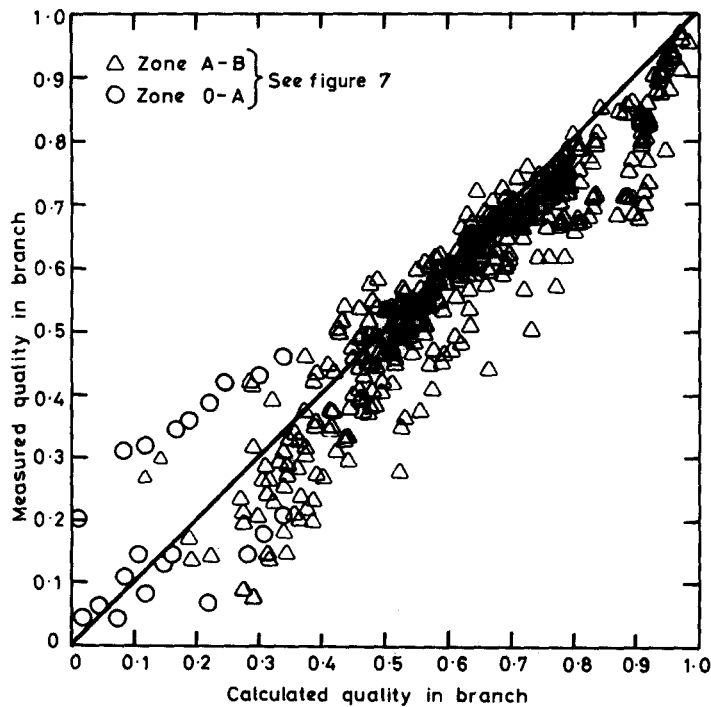
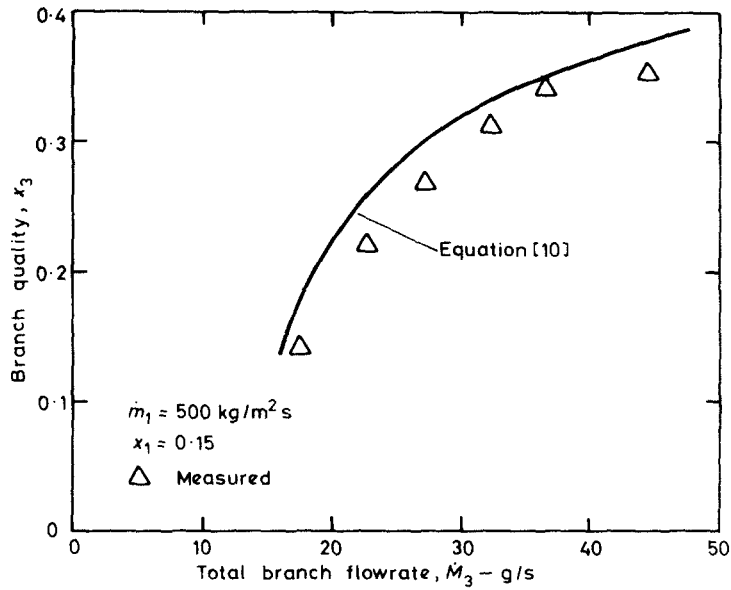
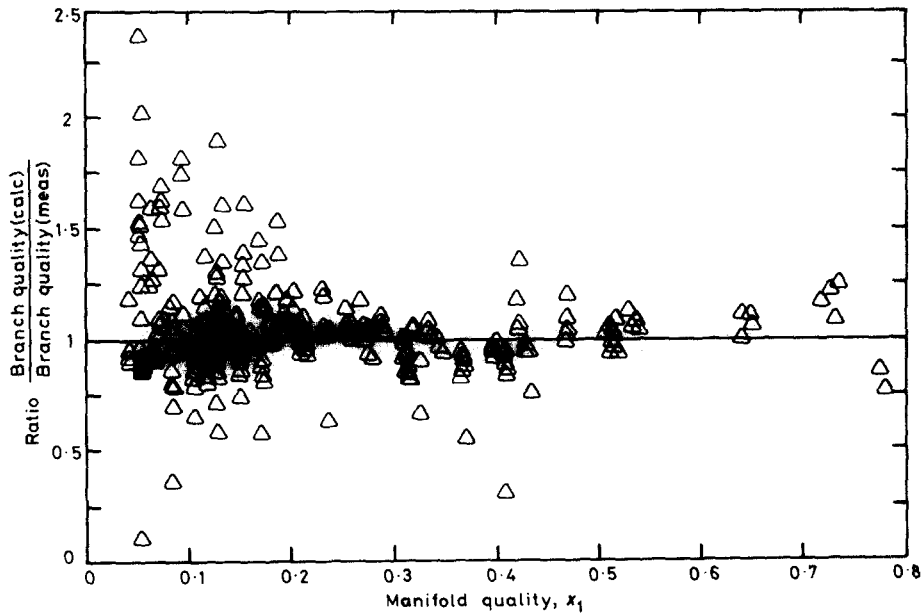


Fig. 11(a).



11(b).



11(c).

Figure 11. Comparison of method with experiment. (a) Agreement for all runs; (b) typical agreement for single test; (c) comparison of calculated and measured branch quality as a function of manifold quality.

Figure 11(c) shows the ratio of calculated branch quality to that measured as a function of the quality in the manifold. The error tends to be greatest at low manifold quality when there is a thick layer of liquid at the bottom of the manifold.

The literature contains very limited data collected in the manner of that reported here. That of Honan & Lahey (1978) is for a rather different geometry and very different flow conditions and cannot be extrapolated for comparison with the present data. However a limited amount of data collected at Harwell has been reported by Collier (1976). This is for a 38-mm dia. manifold with a 25-mm dia. branch, and is compared with the present data in figures 9 and 10. Agreement is reasonable.

6. SIGNIFICANCE OF \dot{m}_i AND S

By definition \dot{M}_i is the liquid flowrate which would be obtained when the branch gas flowrate is zero. This suggests that \dot{M}_i is associated with the flowrate of liquid on the wall of the manifold which is intercepted by the branch opening.

When gas enters the branch it causes (by shear effects) distortion in the liquid film approaching the branch, effectively giving the branch a much larger source of liquid to draw upon. It is also likely that some liquid is carried by the gas in the form of entrained droplets.

Since both \dot{M}_i and S are associated with the structure of the liquid film, it might be expected that they are related to each other. Figure 12 shows that this is so and that for the NEL data the relationship is approx.

$$\dot{m}_i = 50S^{1.33} . \quad [19]$$

Unfortunately no suitable data can be found in the literature to allow the relationship of \dot{m}_i and S to local manifold film conditions to be quantified; this is an obvious line of future research. At present the state of the art is such that it is not possible to calculate, even for settled flow conditions, the liquid distribution within a horizontal manifold. Were this possible it seems likely that a better understanding of T-piece behaviour would result.

7. CONCLUSIONS

(1) Analysis of mixture composition in a branch pipe with two-phase flow has shown that, over a range of quality and mass velocity, the branch component flowrates are related by a linear relationship

$$\dot{M}_{L3} = \dot{M}_i + S\dot{M}_{G3} .$$

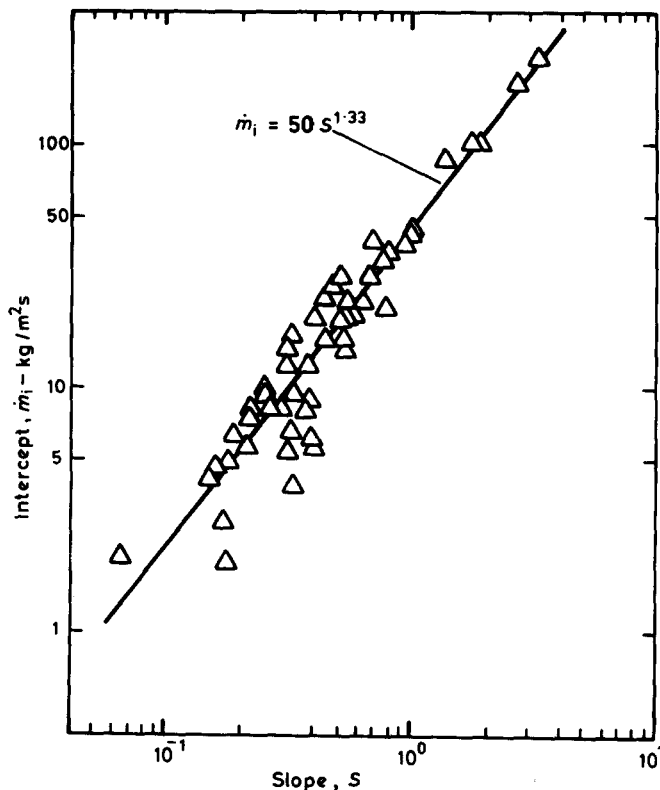


Figure 12. Relationship between \dot{m}_i and S .

(2) For the more annular type of flow pattern the coefficients S and \dot{m}_i can be evaluated by [16] and [17] respectively.

(3) Where the tendency is for the flow to be stratified, the parameter \dot{m}_i is approximately related to the Lockhart–Martinelli parameter by

$$\dot{m}_i = 544 - 491X.$$

(4) Much further work is required to obtain equations or correlations for S and \dot{m}_i for other physical properties and geometries.

(5) Phase behaviour at a branch is very flow pattern dependent. If this could be quantified, for instance by improved computer models, then it seems likely that a better understanding of T-piece behaviour would result.

Acknowledgements—This paper is published by permission of the Director, National Engineering Laboratory, Dept. of Industry. It is Crown copyright reserved. The work reported was supported by the Chemical and Minerals Requirements Board of the Dept. of Industry.

NOTATION

D	manifold diameter, m
d	branch diameter, m
(dp/dz)	frictional pressure gradient, N/m^3
Fr	two-phase Froude number, $Fr = UG_1\sqrt{(\rho_G/(\rho_L - \rho_G)Dg)}$
g	gravitational acceleration m/s^2
K	constant in [1]
K_M	momentum coefficient, [2]
K_S	side-stream coefficient, [3]
M	flowrate, kg/s
\dot{m}	mass velocity, kg/m^2s
\dot{m}_i	branch liquid mass velocity when gas flow is zero, [6], kg/m^2s
n	exponent in [1]
p	pressure, N/m^2
r_3	ratio of total branch flow to total manifold flow
S	slope in [6]
U	velocity, m/s
X	Lockhart–Martinelli parameter $X = \sqrt{((dp/dz)_L/(dp/dz)_G)}$
x	mass quality (gas flow to total flow)
μ	dynamic viscosity, Ns/m^2
π_2	dimensionless gas velocity
ρ	density, kg/m^3
σ	surface tension, N/m

Subscripts

L	liquid
G	gas
1	upstream of branch
2	downstream of branch
3	branch

REFERENCES

- ACRIVOS, A., BABCOCK, B. D. & PIGFORD, R. L. 1959 Flow distribution in manifolds. *Chem. Engng Sci.* **10**, 112–124.

- COLLIER, J. G. 1976 Single-phase and two-phase flow behaviour in primary circuit components. *Two-phase Flows and Heat Transfer*, Vol. I, *Proc. NATO Advanced Study Instit.*, Istanbul, Turkey, 16–27 August.
- DOW, W. M. 1950 The uniform distribution of a fluid flowing through a perforated pipe. *J. Appl. Mech.* **17**, 431–438.
- FOUDA, A. E. 1970 Two-phase annular and annular-mist flows in manifolds. MSc Thesis, Univ. of Waterloo, Ontario, Canada.
- FOUDA, A. E. & RHODES, E. 1972 Two-phase annular flow stream division. *Trans. Instit. Chem. Engrs* **50**, 353–363.
- FOUDA, A. E. & RHODES, E. 1974 Two-phase annular flow stream division in a simple tee. *Trans. Instit. Chem. Engrs* **52**, 354–360.
- HONAN T. J. & LAHEY, R. T. 1978 The measurement of phase separation in wyes and tees. RPI Research Project, 5-24510, Rensselaer Polytechnic Institute, New York.
- HOOPES, J. W., ISAKOFF, S. E., CLARKE, J. J. & DREW, T. B. 1948 Friction losses in screwed iron tees. *Chem. Engng Prog.* **44**, 691–696.
- IDELCHIK, I.E. & SHTEINBERG, M. E. 1974 Formulae, tabular data and recommendations for the choice of gas-, air- and water-distributing headers. *Teploenergetica* **21**, 88–92.
- MARTIN, D. W. & PETERS, G. 1963 The application of Newton's method to network analysis by digital computer. *J. Inst. Water Engrs* **17**, 115–129.
- MARTIN, D. W. & TEE, G. J. 1961 Iterative methods for linear equations with symmetric positive definite matrix. *Computer J.* **4**, 242–254.
- MCNOWN, J. S. 1954 Mechanics of manifold flow. *ASCE Trans.* **119**, 1103–1142.
- MCNOWN, J. S. & HSU, E. Y. 1951 Application of conformal mapping to divided flow. *Proc. Midwestern Conf. Fluid Dynamics*, pp. 143–153. Ann Arbor, Michigan.
- TAITEL, Y. & DUKLER, A. E. 1976 A model for predicting flow regime transitions in horizontal and near horizontal gas–liquid flow. *AIChE J.* **22**, 47–55.
- TSUYNA, M. & TAYA, N. 1959 On the flow of air–water mixture in branch pipes. *Bull. JSME* **2**, 151–156.
- WALLIS, G. B. 1969 *One-dimensional Two-phase Flow*. McGraw-Hill, New York.